

# A Novel-Type Velocity-controllable Electromagnetic Coil Launcher based on Voltage Control

Wenkai Huang<sup>†</sup>, Shi Huan\* and Ying Xiao\*\*

**Abstract** – This paper will present the design of a novel-type velocity-controllable electromagnetic coil launcher (EMCL). By studying the influence of initial capacitor voltage on the velocity of an EMCL, the launcher voltage can be set to precisely adjust the velocity of projectile launching. The simulation of voltage and velocity in relation to time is obtained by Maxwell software. The experimental data show that for the launch accuracy to be achievable, the actual precision is 2%. Because of the excellent performance of Velocity-controllable EMCL, it can replace the air gun and applied to split Hopkinson pressure bar (SHPB).

**Keywords:** Electromagnetic coil launcher, Velocity-controllable, Voltage control

## 1. Introduction

Electromagnetic coil launchers (EMCL) are an important type of electromagnetic launcher. EMCLs have several advantages, including a simple structure, flexible design, and no direct electrical contact between the armature and drive coil, and they have broad application prospects [1-4]. In recent years, much research has been conducted on the performance evaluation and optimization design of EMCLs. In this research area, a simulation method is used to analyze the coil's real-time electromagnetic force, mechanical structure characteristics, manufacturing methods, real-time speed measurement, switch control, and optimal trigger timing, etc. [5-9]. However, little research has been done on the velocity control of EMCL projectiles.

With the development of EMCL applications, some researchers have begun to apply this technology to split Hopkinson pressure bar (SHPB) instead of air guns to launch striker bars. SHPB is used to study the dynamic mechanical properties of materials under one-dimensional stress conditions. The requirements for impact velocity vary depending on the material, especially its ultimate dynamic properties, which are obtained by a precise adjustment of the impact velocity value; therefore, precise control of projectile velocity is required for SHPB applications. The traditional EMCL possesses launch efficiency and maximum emission velocity, but it does not allow accurate control of projectile emission velocity. In [12], the researchers discuss a method of replacing the capacitor group to change the impact velocity. In [10], the relationship between the speed of the striker bar and the capacity of the capacitor is

studied. However, the above studies have not investigated how the accurate controllability of the launching velocity can be realized within a given range.

The effect of charge voltage on the velocity of projectile is studied in this paper, a novel-type velocity-controllable EMCL based on voltage control is proposed. A new circuit that can switch off the current at the appropriate time is designed using an insulated gate bipolar transistor (IGBT), and accurate control of projectile velocity is achieved. The accuracy of the EMCL has been tested, and its launch accuracy was 2%. It met dynamic stress-strain requirements in various experiments with different materials. This attainable method also has a wide range of velocity control because of its cascading multi-stage coils.

## 2. Principle of a Velocity-controllable Emcl based on Voltage Control

The EMCL is essentially a linear motor. Its mechanical structure, shown in Fig. 1, is usually in the form of a barrel, coil, and projectile (i.e., armature). When a pulse current is introduced into the coil, the link flux in the armature induces an opposite ring current, which reverses the drive

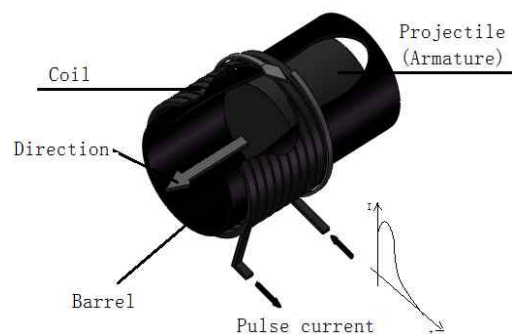


Fig. 1. Schematic diagram of single-stage EMCL

<sup>†</sup> Corresponding Author: School of Mechanical & Electric Engineering, Guangzhou University, Guangzhou, 510006, PR. China. (16796796@qq.com)

\* School of Civil Engineering, Guangzhou University, Guangzhou, 510006, PR. China. (huanshi@263.net)

\*\* School of Mechanical & Electric Engineering, Guangzhou University, Guangzhou, 510006, PR. China. (441339379@qq.com)

Received: August 18, 2017; Accepted: April 24, 2018

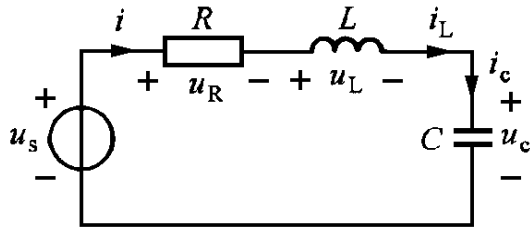


Fig.2. Single-stage EMCL equivalent circuit

current to produce a repulsive Ampere force to drive the armature forward.

When activated, the whole circuit is approximately equivalent to an RLC(resistance, inductor and capacitance) series circuit (Fig. 2).

The whole discharge process can approximate the zero-input response of a second-order circuit and the non-shock discharge process. When the capacitor has been charged,  $u_C = U_0$ ,  $U_0$  is the initial voltage. The initial current in the inductor is  $I_0 = 0$ .

Set the trigger switch and turn on the capacitor group to start the discharge time:  $t = 0$ . According to Kirchhoff's law of voltage (KVL), there is the following:

$$u_C + u_R + u_L = u_s = 0 \tag{1}$$

In the RLC series circuit, the current is as follows:

$$i = i_R = i_L = i_C \tag{2}$$

And the current in a capacitor discharge is as follows:

$$i_C = -C \frac{du_C}{dt} \tag{3}$$

The voltage on the equivalent resistance and inductance is shown in Eq. (4) and Eq. (5).

$$u_R = Ri = -RC \frac{du_C}{dt} \tag{4}$$

$$u_L = L \frac{di}{dt} = -LC \frac{d^2u_C}{dt^2} \tag{5}$$

Substitute Eq. (4) and Eq. (5) into Eq. (1).

$$RC \frac{du_C}{dt} + LC \frac{d^2u_C}{dt^2} + u_C = 0 \tag{6}$$

Eq. (6) is a differential equation of the discharge process of an RLC series circuit with  $u_C$  as an unknown quantity. It is a second-order linear homogeneous differential equation with constant coefficients. Here, by assuming that

$$u_C = Ae^{pt} \tag{7}$$

and by substituting Eq. (7) into Eq. (6), the characteristic

equation can be obtained as follows:

$$LCp^2 + RCp + 1 = 0 \tag{8}$$

The characteristic root is p:

$$p = -\frac{R}{2L} \pm \sqrt{\left(\frac{R}{2L}\right)^2 - \frac{1}{LC}} \tag{9}$$

In Eq. (10), the  $p$  available to the equation has two values:  $p_1$  and  $p_2$ :

$$\begin{cases} p_1 = -\frac{R}{2L} + \sqrt{\left(\frac{R}{2L}\right)^2 - \frac{1}{LC}} \\ p_2 = -\frac{R}{2L} - \sqrt{\left(\frac{R}{2L}\right)^2 - \frac{1}{LC}} \end{cases} \tag{10}$$

The capacitor voltage  $u_C$  is as follows:

$$u_C = A_1e^{p_1t} + A_2e^{p_2t} \tag{11}$$

According to the above equation, the characteristics of root  $p_1$  and  $p_2$  can be known in the loop  $R > 2\sqrt{\frac{L}{C}}$  and the non-oscillatory discharge process for two negative real roots. By Eq. (10),  $p_1$  and  $p_2$  are only related to the circuit structure and parameters and are independent from both the excitation source and the initial energy storage.

When the projectile is launching, the initial condition of the circuit is  $u_C(0_+) = u_C(0_-) = u_C$  and  $i(0_+) = i(0_-) = I_0$ , as a result of the following:

$$i = -C \frac{du_C}{dt} \tag{12}$$

Eq. (12) can obtain Eq. (13):

$$\frac{-I_0}{C} = C \frac{du_C}{dt} \tag{13}$$

From the above initial conditions, Eq. (14) can be obtained:

$$\begin{cases} A_1 + A_2 = U_0 \\ p_1A_1 + p_2A_2 = -\frac{I_0}{C} \end{cases} \tag{14}$$

where  $U_0 \neq 0$  and  $I_0 \neq 0$ .

$$A_1 = \frac{p_2U_0}{p_2 - p_1} \tag{15}$$

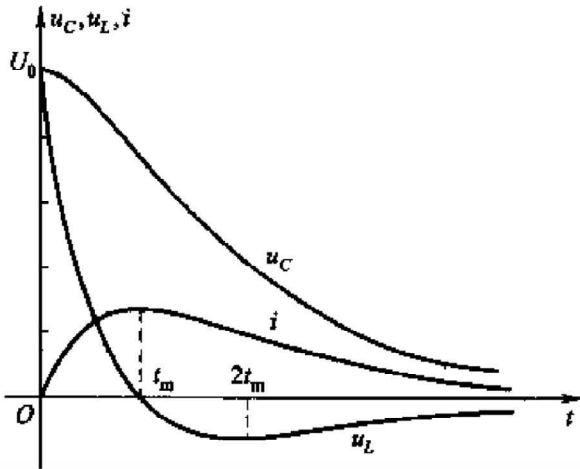


Fig. 3. Time varying curves of  $u_C$ ,  $u_L$ , and  $i$  in non-oscillatory discharges

$$A_2 = \frac{p_1 U_0}{p_2 - p_1} \tag{16}$$

By substituting  $A_1$  and  $A_2$  into Eq. (10), the expression of  $u_C$  can be obtained:

$$u_C = \frac{U_0}{p_2 - p_1} (p_2 e^{p_1 t} - p_1 e^{p_2 t}) \tag{17}$$

A formula for calculating current can then be given, such as Eq. (18) [14]:

$$i = -C \frac{du_C}{dt} = -\frac{CU_0 p_1 p_2}{p_2 - p_1} (e^{p_1 t} - e^{p_2 t}) \tag{18}$$

According to the formula found in [12],

$$F = N^2 i^2 \frac{4g}{\mu_0 \pi d l^2} \tag{19}$$

In Eq. (19),  $N$  is the number of turns of the coil;  $i$  is the coil current;  $g$  is the diameter of the coil and the slot width of the inside of the bullet;  $\mu_0$  is the vacuum permeability;  $d$  is the inner diameter of the c-oil; and  $l$  is the length of the solenoid. The force acting on the projectile in the coil is as follows:

$$F = N^2 \frac{4g}{\mu_0 \pi d l^2} \left[ -\frac{CU_0 p_1 p_2}{p_2 - p_1} (e^{p_1 t} - e^{p_2 t}) \right]^2 \tag{20}$$

It is assumed that the moment the loop current is turned off is  $t_1$  and that the displacement of the projectile in the direction of the electromagnetic force is  $S$  the electromagnetic force of the coil can then be obtained. The work done on the projectile is as follows:

$$W = F \cdot S$$

$$W = \int_0^{t_1} N^2 \frac{4g}{\mu_0 \pi d l^2} \left[ -\frac{CU_0 p_1 p_2}{p_2 - p_1} (e^{p_1 t} - e^{p_2 t}) \right]^2 dt \cdot S \tag{21}$$

The velocity of the projectile at  $t_1$  is determined by the theorem of kinetic energy:

$$v = \sqrt{\frac{2W}{m}}$$

$$= \sqrt{\frac{2 \int_0^{t_1} N^2 \frac{4g}{\mu_0 \pi d l^2} \left[ -\frac{CU_0 p_1 p_2}{p_2 - p_1} (e^{p_1 t} - e^{p_2 t}) \right]^2 dt \cdot S}{m}} \tag{22}$$

According to the Eq. (22), the relation between the velocity of the projectile and the charging voltage of the capacitor can be obtained.

### 3. Implementation of Velocity-controllable Emcl based on Voltage Control

The realization of velocity-controllable EMCL based on voltage control requires a solution to two technical problems: first, to control charging voltage accurately and second, to switch off the circuit at the maximum speed of the projectile.

#### 3.1 Main title and author affiliation

The voltage control circuit uses a high-performance IGBT as the main device and uses a microcontroller unit (MCU) to control the charging rate in real time. The high-frequency switching characteristic of the IGBT can be used to control the charging process of the capacitor. A high-frequency Pulse-Width Modulation (PWM) is used as the control signal of the IGBT [15]. At the same time, the voltage sensor continuously monitors the voltage value of

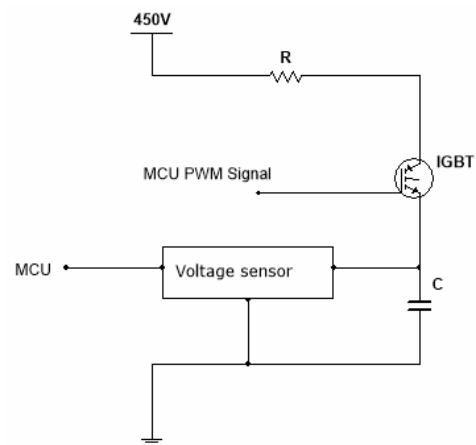


Fig. 4. Charging circuit

the capacitor and sends feedback to the MCU. The MCU adjusts the charge rate in real time through the proportion integral differential (PID) algorithm so that the voltage can be accurately stabilized at the set point. The charging circuit is shown in Fig. 4.

### 3.2 Design of drive coil switch circuit

When the projectile reaches maximum velocity, it is necessary to turn off the circuit in time. Otherwise, the electromagnetic force leads to a decrease in projectile velocity due to the braking nature of the discharge circuit. A metallic oxide semiconductor field effect transistor (MOSFET) is used as a switch control in [10-13], but the specific method of switching the circuit off is not described. When using the MOSFET mentioned in these studies, the circuit can easily burn when the circuit is switched off. In this paper, with the excellent switching characteristic of the IGBT [16], the discharge circuit is switched off at the proper time to reduce the influence of electromagnetic force on the launching velocity of the projectile.

As a power switch, the IGBT generates a higher peak voltage at the moment it is turned off. When the IGBT suddenly turns off, the current will disappear instantly in the inductive load coil circuit. The inductance coil will prevent this mutation in the current, and the induced electromotive force will have a strong current shock on the IGBT. This situation will cause severe avalanche breakdown of the IGBT. Therefore, when the IGBT is used to control the circuit shutoff, the freewheeling diode should be added to the load, as shown in Fig. 5. As to the reverse parallel diode in the inductive energy storage coil, when the voltage or current in the circuit breaks down, the induced electromotive force produced by the coil will be dissipated by the circuit, which is composed of diodes and coils, thus ensuring the safety of other components in the circuit. The IGBT used in this paper is G160N60UFD.

### 3.3 Experiment and analysis

The experimental system that was designed in this paper

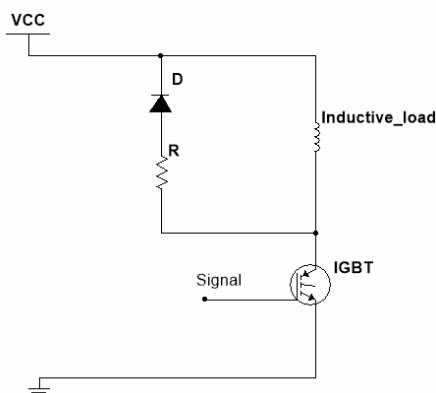


Fig. 5. Drive coil switch circuit

is shown in Fig. 6. The parameters of the system are shown in Table 1.

The repetitive launching accuracy of the EMCL was determined by 10 experiments using the same voltage, and the profile of the launching velocity is shown in Fig. 7. According to the data presented in this Figure, the average velocity, variance, and standard deviation of the 10 experiments at different voltages are calculated, as shown in Table 2. The experimental data show that the launching velocity error of the same voltage is not more than 0.16 m/s, and the control accuracy is 2%.

According to the experimental data, the relationship between the charge voltage and launching velocity shown in Fig. 8 can be obtained. This relationship can be calculated using the conversion between the charge voltage

Table 1. System parameters

Parameters	Unit	Value
Coil turns	turn	300
Coil length	mm	30
Coil inductance	$\mu H$	319.28
Coil outside diameter	mm	25
Coil inside diameter	mm	23
Projectile diameter	mm	8
Projectile length	mm	20
Capacitance	$\mu F$	680
Resistance of discharge circuit	$\Omega$	3.26

Table 2. Experimental results

Category	Capacitor charging voltage (v)															
	100	120	140	160	180	200	220	240	260	280	300	320	340	360	380	
Average velocity (m/s)	5.12	6.40	7.67	8.81	10.00	11.06	12.04	13.00	13.66	14.26	14.81	15.16	15.42	15.72	15.91	
Standard deviation	0.11	0.07	0.16	0.16	0.15	0.15	0.11	0.14	0.09	0.15	0.13	0.11	0.15	0.12	0.13	
Variance	0.11	0.07	0.15	0.14	0.14	0.14	0.11	0.13	0.08	0.14	0.12	0.11	0.14	0.11	0.12	



Fig. 6. Electromagnetic coil launcher

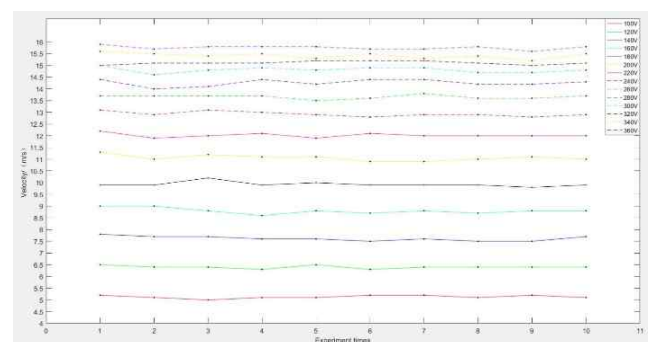
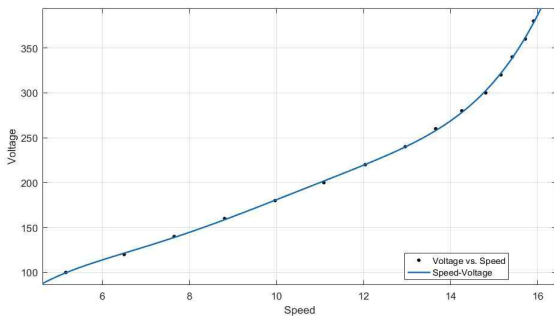


Fig. 7. Distribution of experimental repeatability

**Table 3.** System parameters

Parameters	Unit	Value
Coil turns	turn	350
Coil length	mm	35
Coil inductance	$\mu H$	617.2
Coil outside diameter	mm	46
Coil inside diameter	mm	18
Projectile diameter	mm	16
Projectile length	mm	150
Capacitance	$\mu F$	2,200/1,500
Resistance of discharge circuit	$\Omega$	0.2747



**Fig. 8.** Relationship between charging voltage and launch velocity

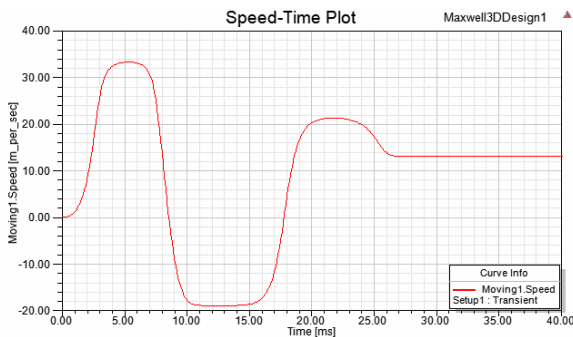


**Fig. 9.** The velocity and time curve of a projectile when the capacity of the capacitance group is 2,200 F

and launching velocity, and accurate control of the launching velocity can be achieved.

### 3.4 Finite element analysis and performance optimization

In order to study the EMCL further by investigating the energy conversion process in the magnetic field of the projectile, finite element analysis of the EMCL is carried out. In this paper, the finite element analysis tool ANSOFT Maxwell 3D is used to simulate the launching process. Moreover, to make our research more practical, we have optimized the parameters of the coil gun, using a coil with larger impedance and current carrying capacity to launch a projectile with larger diameter and longer length. The simulation parameters are shown in Table 3.

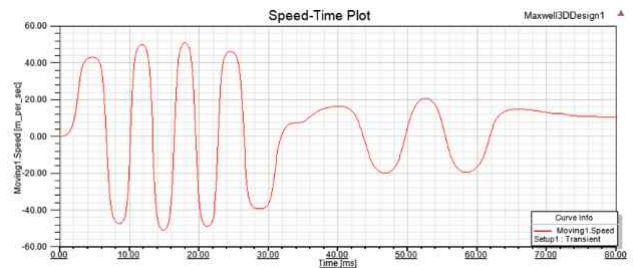


**Fig. 10.** Curve of the velocity and time of a projectile when the capacity of the capacitance is 10 mF

The ferromagnetic projectile is magnetized by the magnetic field generated by the coil, which starts to accelerate its motion. As shown in Fig. 9, the curve of the projectile launch velocity and the time during the launch is shown in the simulation experiment.

From the graph shown above, we can clearly see that the projectile experienced an obvious shock during the launching process, in which it initially accelerated from a standstill to a peak speed of 33.28 m/s, but deceleration began until the projectile reached 0 m/s. Reverse acceleration subsequently propelled it to a peak velocity of -18.86 m/s. Then, the direction of the acceleration process changed again until the projectile reached a final launch speed of 13.06 m/s, which was determined by the properties of the coil gun.

At any moment, the projectile coils can pull to the center of the coil. The energy stored in the capacitive group after the projectile geometry center passes through the coil geometry center is not completely released. There is still a large current flowing through the coil, and the generated magnetic field is negative work of the projectile back to the coil, until the energy of the capacitance group is released.

We verified this theory by another simulation experiment. With the other parameters unchanged, we increased the capacity of the capacitor to 10 mF to make the oscillation more obvious. The relationship between the velocity and time of the projectile is shown in Fig. 10.

To improve the launch speed and efficiency of a projectile, it is necessary to match the appropriate capacitance group capacity to control the launching speed better by adjusting the initial voltage of the capacitor bank. Without changing the other parameters of the coil, we find that when the capacitance is 1,500 $\mu F$ , the energy of the coil is released almost exactly at and through the geometric center of the projectile, and the launch efficiency is significantly improved. The velocity and time curve of the projectile is shown in Fig. 11.

In Fig. 11, the velocity of the projectile drops only slightly after its peak and then stabilizes.

We have done a more thorough study of this small detail. After becoming magnetized, the projectile is magnetically accelerated, and the moving magnetic field will induce the back electromotive force (EMF) in the coil to prevent projectile motion and reduce its velocity. As the projectile

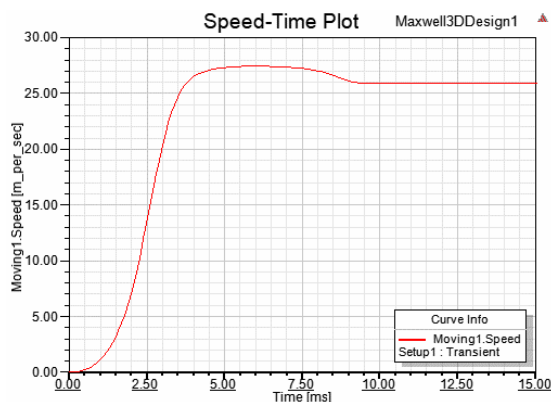


Fig. 11. The velocity and time curve of a projectile when the capacity of the capacitance is 1,500  $\mu\text{F}$

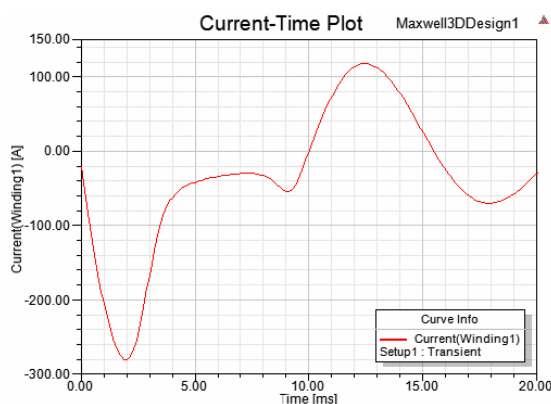


Fig. 12. The relationship between current and time in the coil during the launching process

is magnetized, this back EMF begins to move and is maintained throughout the entire process, until the projectile is completely removed from the influence of the coil.

Fig. 12 is a graph of the launching process detailing the coil current and time. The initial emission current is mainly composed of capacitor voltage poles, with small back EMF. When the launching process continues, the capacitor voltage decreases; eventually, the EMF gains an advantage, with the projectile speed increasing slowly. After a slight reduction followed by a peak, it finally stabilizes.

Through several simulation experiments, it is found that by reasonably optimizing the coil parameters and the control method, the launching velocity of projectiles can be controlled more safely, accurately, and effectively.

#### 4. Conclusion

In this paper, an EMCL based on voltage control is designed, which can control the launching velocity and satisfy the application of SHPB, or a similar application,

which requires the velocity of launching to be controlled. The experimental verification of single-stage EMCL is carried out, and the controllability of multi-stage EMCL will be verified in the future, along with the independent voltage control of different coils. We hope to develop a velocity-controllable EMCL with higher precision and a wider range of control.

#### Declaration of conflicting interests

The author(s) declared no potential conflicts of interest with respect to the research, authorship, and/or publication of this article.

#### Acknowledgements

The author(s) disclosed receipt of the following financial support for the research, authorship, and/or publication of this article: This work was supported by the scientific research projects of Guangzhou municipal colleges and Universities (Grant No. 1201620371).

#### References

- [1] R. Haghmaram and A. Shoulaie, "Literature review of theory and technology of air-core tubular linear induction motors [electromagnetic launcher applications]," in *39th International Universities Power Engineering Conference*, 2004, pp. 517-522.
- [2] K. Y. Zhao et al., "Finite element analysis of magnetic field and eddy field in synchronous induction coil-gun," *High Voltage Engineering*, vol. 34, no. 3, pp. 492-495, 2008.
- [3] M. S. Aubuchon et al., "Results from Sandia National Laboratories/Lockheed Martin electromagnetic missile launcher (EMML)," in *IEEE Pulsed Power Conference*, 2005, pp. 75-78.
- [4] M. S. Aubuchon et al., "Study of coilgun performance and comments on armatures," in *Power Modulator Symposium, and High-Voltage Workshop, Conference Record of the Twenty-Sixth International*, 2004, pp. 141-144.
- [5] Y. D. Zhang et al., "Mechanical property and manufacture technology of electromagnetic driving coil," *High Voltage Engineering*, vol. 40, no. 4, pp. 1186-1193, 2014.
- [6] X. Li, Q. L. Wang, and J. J. Liu, "Optimization and analysis of linear induction launcher," *Advanced Technology of Electrical Engineering and Energy*, vol. 29, no. 2, pp. 43-47, 2010.
- [7] H. D. Fair, "Guest editorial: The past, present, and future of electromagnetic launch technology and the IEEE International EML Symposia," *IEEE Transactions on Plasma Science*, vol. 41, no. 5, pp. 11-16,

- 2013.
- [8] M. Wang et al., "Trigger control research of electromagnetic coil launcher based on real-time velocity measurement," *IEEE Transactions on Plasma Science*, vol. 44, no. 5, pp. 885-888, 2016.
  - [9] F. C. Li, B. Lei, and Z.Y. Li, "Dynamic simulation and experiment research on the single-stage induction coil-launcher," *Micromotors*, vol. 43, no. 11, pp. 37-41, 2010.
  - [10] W. G. Guo et al., "Electromagnetic Driving Technique Applied to Split-Hopkinson Pressure Bar Device," *Journal of Experimental Mechanics*, vol. 25, no. 6, pp. 682-689, 2010.
  - [11] Z. W. Liu et al., "On the Mini-SHPB Device Based on Multi-level electromagnetic Emissions," *Journal of Experimental Mechanics*, vol. 28, no. 5, pp. 557-562, 2013.
  - [12] Z. W. Liu et al., "The Optimization of Multi-stage Electromagnetic launching System of MiniSHB," *Journal of Experimental Mechanics*, vol. 30, no. 1, pp. 9-16, 2015.
  - [13] W.G. Guo, Concise course of stress wave. Shanxi: Northwestern Polytechnical University Press, 2007.
  - [14] G.Y. Qiu circuit, fifth edition. Beijing: Higher Education Press, pp. 156-158, 2006.
  - [15] Baharlou, S et al. "A Non-Isolated High Step-up DC/DC Converter with Low EMI and Voltage Stress for Renewable Energy Applications," *Journal of Electrical Engineering & Technology*, vol. 12, no. 5, pp. 1187-1194, 2017.
  - [16] Bae, S et al., "A Study on SFCL with IGBT Based DC Circuit Breaker in Electric Power Grid," *Journal of Electrical Engineering & Technology*, vol. 12, no. 5, pp. 1805-1811, 2017.



**Ying Xiao** He is currently junior student in Guangzhou University. His research interests include electromagnetic emission and distributed parameter system control.



**Wenkai Huang** He was born in Guangdong, China. He received his B.S degree and M.S. from Guangdong university of Technology. He received his Ph.D. degree from Guangzhou University. His research interests are robust control, impact dynamics and robotics.



**Shi Huan** He received his B.S degree from University of Science and Technology of China. He received his M.S degree from National University of Defense Technology. He received his Ph.D. degree from Beijing Institute of Technology. His research interests are civil engineering protection, structural

health monitoring, and impact dynamics.